Optica Applicata, Vol. XI, No. 1, 1981

Optical noises in amplitude holography, developed by nonlinear properties of recording media

TADEUSZ LIPOWIECKI
Technical University of Radom, Radom, Poland.

Optical noise effects arising when holographic signals are recorded in nonlinear amplitude media are discussed in the paper. It has been pointed out that holograms generate a number of disturbing signals, possessing the same spatial frequency ranges as the desired signal. The possibilities of determining separately the powers of the noise and desired signals are discussed. The method discussed was applied to execute the experimental measurements. The results of diffraction efficiency measurements for holograms are presented with respect to the desired signal alone and the signal-to-noise ratio. Some general conclusions valid of all domains of amplitude holography are discussed.

1. Introduction

In all the cases when desired signals are disturbed by the not desired ones, we can speak about the presence of noises. In conventional optics the sources of optical noises, like scattering at surfaces, and in volumes, inhomogeneity and turbulence effects, reflections and outside light sources and so forth are very well known. In coherent light optics some new sources of noises appear, like diffraction and interference patterns, developed by scattering of coherent light at particles, randomly diffusing objects and others.

In holography quite new sources of undesired signals are encountered, i.e. nonlinear properties of recording media. Due to nonlinear effects the holograms generate not only the desired signals, but also a number of the undesired ones. The general aim of this report is to show, how these undesired signals arise in amplitude holograms. Moreover, some practical suggestions can be concluding from the presented results of measurements which allow to establish the conditions of hologram exposure in the cases of alternative situations when a compromise between the diffraction efficiency and the noise level occurs.

2. Holographic signals and recording conditions

Let us consider a general holographic example, where two coherent waves u and u_0 propagate and interfere in space (fig. 1). If we assume that polarizations of the two waves are planar and of the same direction and, moreover,

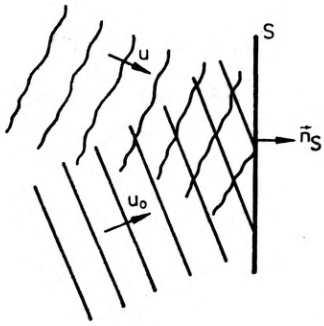

Fig. 1. Holographic recording of a power density distribution created by two incident coherent waves

that the angles between normal to the phase fronts and the plane S vectors are small enough, then the scalar representation can be used in the description of the electromagnetic fields. The designations u and u_0 represent amplitude and phase distributions of the waves vs. space coordinates:

$$u = \bar{u}(x, y, z) \cdot \exp[i\varphi(x, y, z)], \tag{1}$$

$$u_0 = \bar{u}_0(x, y, z) \cdot \exp[i\varphi_0(x, y, z)]. \tag{2}$$

Here, the time dependent factor $\exp(i\omega t)$ is omitted.

Spatial power density distribution $P(x, y, z)$ can be written as

$$P(x, y, z) = \frac{1}{2z_v}(u + u_0)(u^* + u_0^*) = \frac{1}{2z_v}(\bar{u}_0^2 + \bar{u}^2 + u_0^* u + u u_0^*), \tag{3}$$

where z_v — the wave impedance of the free space. The components $\bar{u}_0^2$ and $\bar{u}^2$ are real values, the sum $u_0^* u + u_0 u^*$ is a real value too, and can be written as

$$u_0^* u + u_0 u^* = 2\bar{u}_0 \bar{u} \cos(\varphi_0 - \varphi). \tag{4}$$

If a photosensitive layer, the recording properties of which are represented by the characteristic T_a vs. H, with H equal to

$$H = P \cdot t, \tag{5}$$

is placed in the plane S, then the amplitude transmittance distribution in this plane may be written generally as

$$T_a(x, y, z)|_S = T_a\{H[P(x, y, z)|_S]\}. \tag{6}$$

When there is a linear dependence between T_a and H, the amplitude distribution (6) corresponds to the power density distribution (3). In reproduction process, when the plane S is illuminated solely by the wave u_0, we get the following assembly of the generated waves

$$u_{\text{gen}} = \text{const}(\bar{u}_0^2 u_0 + \bar{u}_a^2 u_0 + \bar{u}^2 u + u_0^2 u^*). \tag{7}$$

Let us assume that the value of the amplitude $\bar{u}_0$ is constant. The third and fourth components of (7) represent two first-order waves diffracted on the interference structure, which resulted from the interference between the waves u and u_0. The component $\bar{u}_0^2 u$ corresponds to the original wave u. If the separation conditions, which will be discussed later, are satisfied, then the wave $\bar{u}_0^2 u$ may be separated from the three others.

The first and the second components of (7) represent the zero-order diffracted wave. The first one does not change the amplitude distribution of the illuminating wave u — it has a homogeneous absorbing filter property. The second component contains the factor $\bar{u}^2$, which represents a certain self-interference spatial structure of the wave u in the plane S. In general, although the function $\bar{u}^2|_S$ changes much more slowly in the plane S than the sum (4), it nevertheless produces diffraction of the wave u and — after passing it through the amplitude modulator in the plane S — it consequently causes its angular divergence. In order to define the field distribution of the diffracted wave in the half-space after the modulator, we ought to know the explicit function $u(x, y, z)|_S$, then to take its square and finally — using the Helmholtz–Kirchhoff's integral formula — to define the explicit function of the diffracted wave vs. coordinates x, y, and z. Such a procedure is a mathematical formalism only, because under such complex boundary conditions neither the distribution $u(x, y, z)|_S$ is in general known nor the integral of Helmholtz–Kirchhoff's formula is solvable.

Let us determine a simple configuration of a holographic recording geometry, which — being the most convenient for mathematical descriptions — would not lose the physical meaning of the phenomena. A simplified holographic scheme is shown in fig. 2. Let the following assumptions be taken with respect to this scheme:

— an object is a segment of a straight line,
— the luminance of the object is uniformly distributed,
— the boundary angles α_1 and α_2 are so small that the following

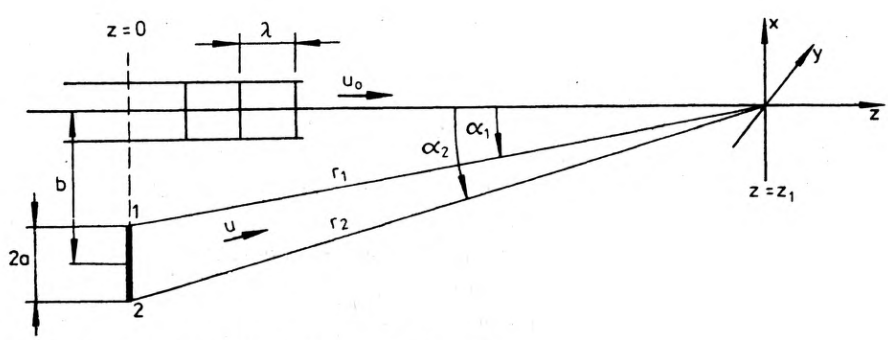

Fig. 2. A simplified holographic recording scheme

approximation is valid

$$\sin\alpha \cong \alpha \cong \tan\alpha, \tag{8}$$

— the incidence angle of the reference wave u_0 is equal to zero, hence

$$u_0 = u_0^*, \tag{9}$$

— recording conditions are confined to a small region of the recording surface in the surrounding of the point $x = y = 0$, $z = z_1$.

Every point of the object can be treated as an elementary source of a spherical wave of the length λ. If we assume that its phase front in a close surrounding of the point $x = y = 0$, $z = z_1$, may be treated as a planar one, then frequency, with which the constant and equal phase planes of this wave intersect the recording plane $z = z_1$, can be defined as follows

$$f_x = \frac{\sin\alpha}{\lambda} \cong \frac{\alpha}{\lambda} = \frac{x}{\lambda z_1}, \tag{10}$$

where x is the coordinate of the object in the plane $z = 0$. Since, according to our assumptions, the distances r_1 and r_2 are near each other, then the information wave in the discussed recording region may be represented by a spectrum of plane waves $\hat{U}(\omega_x)$, with a constant amplitude distribution $U(\omega_x)$ and a pass-band frequency range, ranging within the limits:

$$\frac{b-a}{\lambda z_1} \leqslant \frac{\omega_x}{2\pi} \leqslant \frac{b+a}{\lambda z_1}. \tag{11}$$

Thus we have got a spectral representation of the information signal in the plane z_1.

Now, the general line of our consideration will be the following: in fact, the positional representation $u(x, y, z)$ of the information wave is not known, but we can suppose that it is given in explicit form. If the recording properties of the photosensitive medium are represented by the power-series approximation

$$T_a = T_{a_0} + \sum_{m=1}^{n} k_m H^m, \tag{12}$$

then the amplitude transmittance distribution $T_a(x, y, z_1)$ will also be represented in the form of a power-series. The components of this series will contain the products of u_0, u and u^*. Each component will generate a characteristic wave. We are interested in the amplitudes and propagation directions of these waves — they are contained in spectral representations of the waves. Thus, by denoting the spectral representations of each component of the power-series distribution $T_a(x, y, z_1)$, we shall get the final answer to our problem.

Positional and spectral representations of the same signal are interrelated through the well known Fourier transformation. One of the properties of this transformation is the following

$$\mathcal{F}[f_1(x)\cdot f_2(x)] = \frac{1}{\sqrt{2\pi}}\mathcal{F}_1(\omega)\otimes\mathcal{F}_2(\omega) \tag{13}$$

and symmetrically

$$\mathcal{F}[\mathcal{F}_1(\omega)\cdot\mathcal{F}_2(\omega)] = \frac{1}{\sqrt{2\pi}}f_1(x)\otimes f_2(x). \tag{14}$$

Functions $\mathcal{F}_1(\omega)$ and $\mathcal{F}_2(\omega)$ are spectral representations of the signals, written in positional representations $f_1(x)$ and $f_2(x)$, respectively. The symbol $\otimes$ denotes the convolution operation

$$f(x) = f_1(x)\otimes f_2(x) = \int_{-\infty}^{+\infty} f_1(x-\xi)f_2(\xi)\,d\xi. \tag{15}$$

Graphical representation of a convolution of two simple functions is shown in fig. 3.

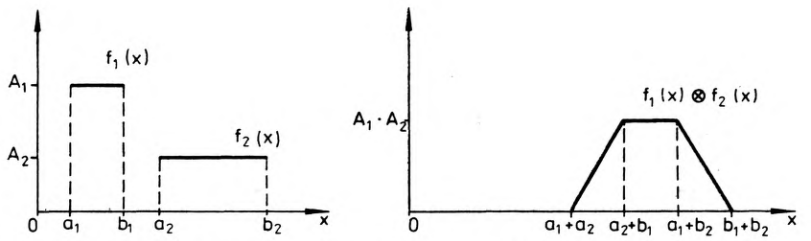

Fig. 3. Graphical representation of the convolution of two functions

Now, let us return to the situation presented in fig. 2. Let us suppose that recording properties of a photosensitive medium in the exploited range may be approximated as

$$T_a = T_{a_0} + k_1 H + k_2 H^2. \tag{16}$$

Taking (3), (5), and (9) into account and inserting them into (16), the following representation of the amplitude transmittance T_a is obtained

$$T_a = T_{a_0} + c_1 u_0^2 + c_2 u_0^4 \tag{17a}$$

$$+ (c_1 + 4c_2 u_0^2)\cdot |u|^2 + c_2 |u|^4 \tag{17b}$$

$$+ (c_1 u_0 + 2c_2 u_0^3)(u + u^*) \tag{17c}$$

$$+ 2c_2 u_0 |u|^2 (u + u^*) \tag{17d}$$

$$+ c_2 u_0^2 (u^2 + u^{*2}), \tag{17e}$$

where

$$c_m = k_m \left(\frac{t}{2z_r}\right)^m. \tag{18}$$

Each component in relation (17) generates a diffracted wave characteristic of this component. The amplitude and directional properties of each wave can be estimated by calculating a multiconvolution function of the corresponding product with respect to u_0, u and u^*. In our case the spatial representation of the reference wave u is simply the δ-Dirac distribution $U_0\delta(\omega = 0)$, so — on account of its selective properties — it does not influence the amplitude and phase distributions. In view of this fact the spatial frequency representations of all the waves are defined by multiconvolution functions concerning the spatial frequency representations of u and u^*, for instance

$$\mathcal{F}[|u|^2 u^*] = \mathcal{F}[u u^* u^*] = \hat{U}(\omega) \otimes U^*(-\omega) \otimes U^*(-\omega). \tag{19}$$

The spectral representations of the optical signals corresponding to the geometrical configuration presented in fig. 2 are shown in fig. 4. The

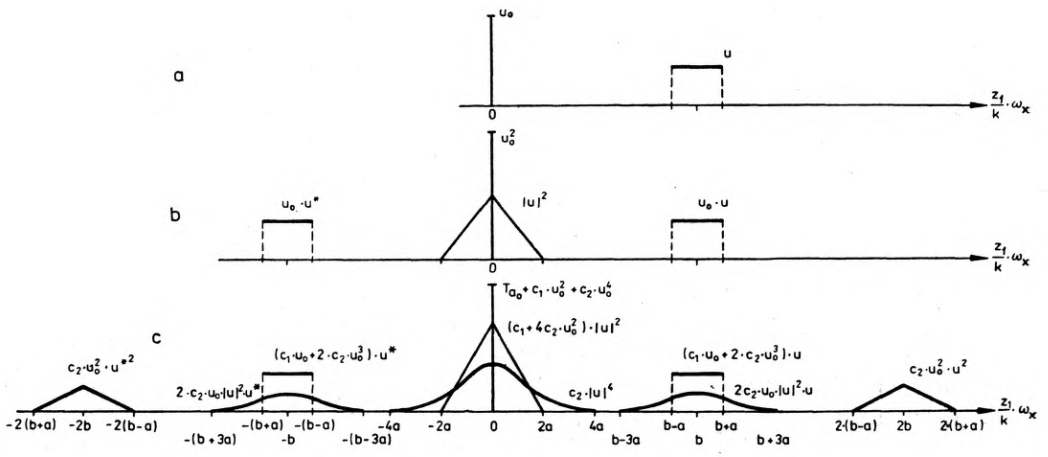

Fig. 4. Spectral representation of the holographic signals related to the configuration shown in fig. 2:
a — amplitude spectrum of the recorded waves,
b — amplitude spectrum of the generated waves — linear recording conditions,
c — amplitude spectrum of the general waves — nonlinear, second power recording conditions

spatial frequency coordinates have been normalized in such a way to get a direct correspondence to the dimensions a and b, in fig. 2. Figure 4a presents the amplitude spectrum of the waves u_0 and u, fig. 4b — the amplitude spectrum of the waves generated by a hologram when linear recording conditions are maintained. In fig. 4c we can see the amplitude

spectrum of all the waves corresponding to all the components of the relation (17), which have been obtained in the case of the parabolic approximation (16) of the properties of the recording medium.

Separation conditions, mentioned before, follow directly from the situation presented in fig. 4. As it can be seen, the spectral separation between the desired signal u and the zero-order diffracted signals will be kept if the highest spatial frequency of the zero-order waves is lower than the lowest spatial frequency of the desired signal wave u. In the case of linear recording conditions it is sufficient that

$$b \geqslant 3a. \tag{20}$$

In nonlinear recording conditions more rigorous constraints ought to be anticipated.

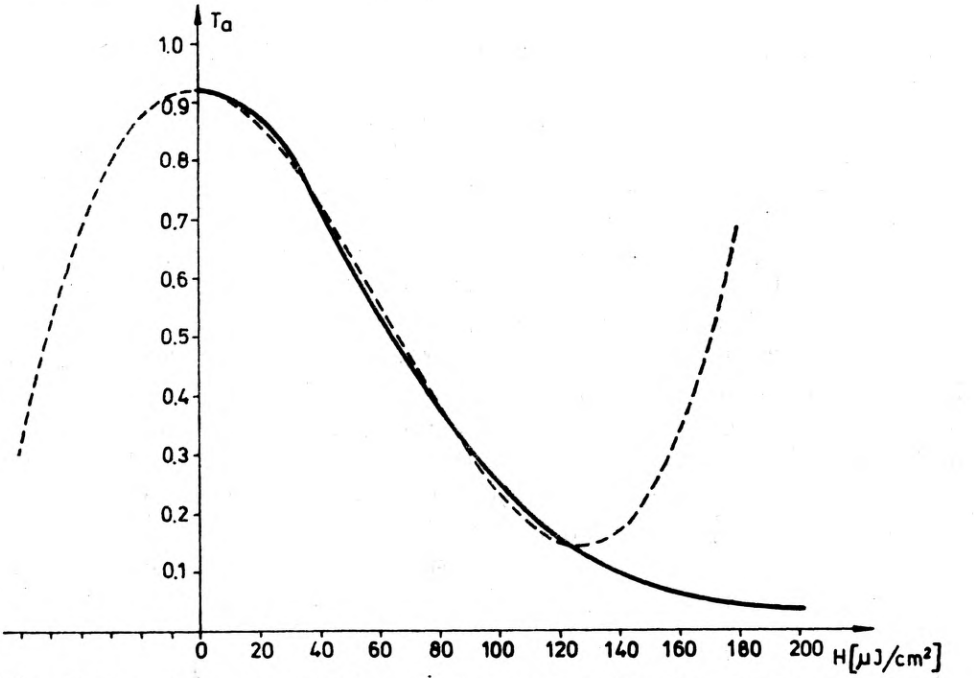

Fig. 5. The real characteristic $T_a - H$ of the holographic plates 649F and its approximation by a third-power polynomial

In fact, the second-power approximation of the $T_a - H$ characteristic is not sufficient in many cases of the holographic practice. Figure 5 present the real shape of the $T_a - H$ characteristic of the Kodak 649F holographic plates and its approximation by the third-power polynomial

$$T_a = 0.92 - (0.573 \times 10^{-3})H - (0.137 \times 10^{-3})H^2 + (0.753 \times 10^{-6})H^3, \tag{21}$$

where the exposure H is described in $\mu J/cm^2$ units. In all the cases when the

polynomial applied as an approximation functional is of the degree higher than the second power (16), a number of distrubing signals will appear, whose spatial frequency range is the same range of the desired signal. Simple mathematical calculations lead to the recurrent relation which describes all the disturbing component waves

$$T_{a_1} = u_0 u \sum_{m=1}^{n} m c_m (u_0^2 + |u|^2)^{m-1} \tag{22}$$

with the assumption

$$u_0 = u_0^* = \text{const}.$$

3. Possibilities to determining the signal-to-noise ratio

In chapter 2 the general idea of disturbing signal generation in holographic processing has been presented. In order to determine the signal-to-noise ratio (SNR) in an analytic form, we ought to know:

— an analytical description of the nonlinear medium properties,

— statistical properties of the information wave field,

— the values determining recording conditions, i.e. the exposure time and the ratio of the average power density of the information wave to the power density of the reference wave.

Obviously, it is not possible in practice to get any digital data in an analytic way. The answers to questions of interest may be solely provided by experimental investigations.

In determining the SNR the basic problem is how to separate the desired signals from the noise ones, if their spatial frequencies fall into the same range. In experimental investigations we must take not an ideal one-dimensional object, as in fig. 2, but at least two-dimensional one, like a square or a circle. Let us arrange the simple holographic recording scheme with a two-dimensional object, as shown in fig. 6. The object

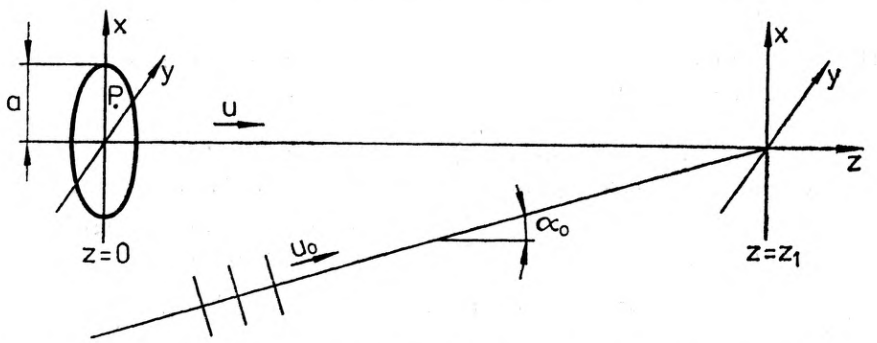

Fig. 6. A simple holographic recording scheme with a two-dimensional object

of a circular symmetry is positioned in the plane $z = 0$, the position of the recording plane corresponds to $z = z_1$. Our considerations will follow these in chapter 2: every point of the object surface can be treated as an elementary source of a spherical wave. In small surrounding of the centre point in the recording plane these waves can be treated as the planar ones. The inclination of each elementary wave front to the plane z_1 is determined by two spatial frequencies

$$\omega_x = 2\pi x/\lambda z_1, \qquad \omega_y = 2\pi y/\lambda z_1, \tag{23}$$

where x and y are the object coordinates. If the distance d between the point P in the object plane and the centre point of the recording plane obeys the approximation

$$d = \sqrt{x^2+y^2+z_1^2} \cong z_1, \tag{24}$$

then the amplitude distribution $U(\omega_x, \omega_y)|_{z_1}$ corresponds to the amplitude distribution $\bar{u}(x, y)|_{z=0}$ with the accuracy of a constant coefficient. If nonlinear recording properties of the recording medium are represented by a power-series polynomial like (12), then we can estimate the spectral representations of disturbing signals with appropriate two-dimensional multiple-convolutions of $U_0 \cdot \delta(\omega_{0_x})$ and $U(\omega_x, \omega_y)$. Such a mathematical procedure does not lead, in general, to any analytic solution. In order to solve this two-dimensional problem, two following assumptions were taken:

1. The amplitude distribution of the information wave at the object surface is of a circular symmetry:

$$\bar{u}(x, y)|_{z=0} = \bar{u}(r)|_{z=0}, \tag{25}$$

where

$$r = \sqrt{x^2+y^2}. \tag{26}$$

2. The explicit description of the distribution (25) is a Gaussian function.

The first assumption substantially simplifies our considerations, reducing a two-dimensional problem to the one-dimensional one; it is so because the two-dimensional Fourier transformation of circular symmetry functions changes itself into the one-dimensional Hankel transformation, defined as follow

$$\left.\begin{aligned} \mathcal{H}(\omega) &= \int_0^\infty f(r)\cdot r\cdot J_0(\omega\cdot r)\cdot dr \\ f(r) &= \int_0^\infty f(\omega)\cdot \omega\cdot J_0(\omega\cdot r)\cdot d\omega \end{aligned}\right\}, \tag{27}$$

where J_0 is the Bessel function of the zero-order, $f(r)$ and $\mathscr{H}(\omega)$ are positional and spectral representations of the same signal. All the other properties of the Hankel transformation, especially with respect to convolutions and their transformations, are the same as in the case of the one-dimensional Fourier transformation.

The second assumption was made because of unique properties of the Gaussian distribution — it conserves its Gaussian character even, if it is transformed into another representation or is multiconvoluted with itself.

Now we can trace the ground plane of our considerations. The amplitude distribution of the information wave in the object plane is assumed to be

$$\bar{u}(r, z = 0) = \bar{u}(0, 0)\exp[-(r/w_S)^2], \tag{28}$$

where w_S is the amplitude norm of the Gaussian distribution. The spectral representation of the information wave in the centre of the z_1 plane is determined as

$$U(\omega, z_1) = \text{const}\cdot\exp[-(\omega/\omega_S)^2], \tag{29}$$

where

$$\omega_S = 2\pi w_S/\lambda z_1. \tag{30}$$

There may arise some constraints as to the reference wave u_0 which —in the cases when its incidence angle α is not equal to zero —does not possess a circular symmetry and, consequently, its Hankel transformation does not exist. As a matter of fact, the components of the diffracted wave which belong to the first-order direction and create disturbing signals are known exactly from (22). Thus, in our considerations we can put the angle $\alpha = 0$ and assume that the Hankel spectral representation of the reference wave is equal to $\text{const}\cdot\delta(\omega = 0)$. In practice the inclination of the reference wave separates the waves of the individual orders only, as it is shown in fig. 4c.

Spectral representations of the disturbing signals are determined by the appropriate multiple auto-convolutions of the relation (29), corresponding to the components included in the relation (22). As can be simply derived, the Hankel transformation of the multiple auto-convolution of the spectral representation $U(\omega, z_1)$ is equal — within the accuracy to a constant value — to the n-th power of the Hankel transformation of the same function $U(\omega, z_1)$:

$$\mathscr{H}\{[U(\omega, z_1)]^{\otimes n}\} = \text{const}\cdot\{\mathscr{H}[U(\omega, z_1]\}^n. \tag{31}$$

In general, the Hankel transformation of a Gaussian function is

$$\mathcal{H}[\exp(-a\omega^2)] = \frac{1}{2a}\cdot\exp(-r^2/4a). \tag{32}$$

Taking into account (29) and (32) we obtain

$$\mathcal{H}\{[U(\omega, z_1)]^{\otimes n}\} = \text{const}\cdot\exp\left[-\left(\frac{\sqrt{n}\,r\,\omega_S}{2}\right)^2\right]. \tag{33}$$

From symmetrical properties of the relation (27) it follows that

$$\mathcal{H}\{\mathcal{H}[f(r)]\} = f(r). \tag{34}$$

Thus, if we transform both sides of the relation (33), we obtain

$$[U(\omega, z_1)]^{\otimes n} = \text{const}\cdot\exp\left[-\left(\frac{\omega}{\sqrt{n}\,\omega_S}\right)^2\right]. \tag{35}$$

Let us notice, that numbering index n in the relation (22) does not correspond to the index n in the relation (35). As it follows from (22), the powers of the u distribution are successive odd numbers changing from unity to $2n-1$, where n denotes the power of the approximating polynomial, accordingly the index n in (35) runs through the odd values from unity to $2n-1$. For $n=1$ we get the spectral representation of the desired signal, for $n = 3, 5, \ldots, 2n-1$ — the spectral representations of all noise signals. Following the reverse consideration with respect to elementary convergent spherical waves, and creating now the amplitude distributions in the object plane, we obtain the positional representation of reproduced waves

$$\bar{u}_S(r) = \bar{u}_S(0)\cdot\exp[-(r/w_S)^2], \tag{36}$$

$$\bar{u}_{N_1}(r) = \bar{u}_{N_1}(0)\cdot\exp[-(r/\sqrt{3}w_S)^2], \tag{37a}$$

$$\bar{u}_{N_2}(r) = \bar{u}_{N_2}(0)\cdot\exp[-(r/\sqrt{5}w_S)^2], \tag{37b}$$

and so forth.

The corresponding power density distributions are:

$$p_S(r) = p_S(0)\cdot\exp[-(r/r_w)^2], \tag{38}$$

$$p_{N_1}(r) = p_{N_1}(0)\cdot\exp[-(r/\sqrt{3}r_S)^2], \tag{39a}$$

$$p_{N_2}(r) = p_{N_2}(0)\cdot\exp[-(r/\sqrt{5}r_S)^2], \tag{39b}$$

and so forth.

The norm r_w is

$$r_w = w_S/\sqrt{2}. \tag{40}$$

In order to determine the total power of every power density distribution, let us at first calculate the integral

$$\int_S \exp(-ar^2)\cdot dS = \int_0^\infty r\cdot\exp(-ar^2)\cdot dr \int_0^{2\pi} d\Theta = 2\pi \int_0^\infty r\cdot\exp(-ar^2)\cdot dr.$$

Introducing a new variable $\varrho = a\cdot r^2$ we get

$$\int_S \exp(-ar^2)\cdot dS = \frac{\pi}{a}\int_0^\infty \exp(-\varrho)d\varrho = \frac{\pi}{a}.$$

Because the value $1/a$ corresponds to the values r_w^2, $3r_w^2$ and so forth, we get the total power of every component:

$$P_S = \pi r_w^2 p_S(0), \tag{41}$$

$$P_{N_1} = 3\pi r_w^2 p_{N_1}(0), \tag{42a}$$

$$P_{N_2} = 5\pi r_w^2 p_{N_2}(0), \tag{42b}$$

and so forth.

Finally, we can determine the signal-to-noise ratio:

$$\mathrm{SNR} = P_S / \sum_i P_{N_i} = \frac{p_S(0)}{3p_{N_1}(0)+5p_{N_2}(0)+\ldots}. \tag{43}$$

4. Experimental measurements of the signal-to-noise ratio

In order to determine the SNR in holographic process, first the separate powers of the desired and noise signals should be found. As it was shown in chapter 3, if the exploited range of the amplitude transmittance characteristic $T_a - H$ is described with a sufficient accuracy by an n-th power polynomial and if the power density distribution of the information wave in the object plane is a Gaussian one with the norm r_w, then in the reproducing process we obtain an assembly of Gaussian distributions

$$\begin{aligned} p(r) &= p_S(r)+p_{N_1}(r)+\ldots+p_{N_{n-1}}(r) \\ &= p_S(0)\cdot\exp[-(r/r_w)^2]+p_{N_1}(0)\cdot\exp[-(r/\sqrt{3}r_w)^2]+\ldots \\ &\quad +p_{N_{n-1}}(0)\cdot\exp[-(r/\sqrt{2n-1}r_w)^2]. \end{aligned} \tag{44}$$

Measuring the values $p(r_k)$ at n different values of r_k we can obtain a pattern of n linear equations, where the power densities $p_S(0)$ and $p_{N_i}(0)$ are the unknown variables. Such a procedure, however, leads to some troubles concerning especially the accuracy of measurements in cases when noise levels are low and comparable with the measurement error. In order to

avoid this difficulty in the recording process a circular diaphragm with a radius a was applied in the object plane. The general sense of the limiting diaphragm application is the following: if the relative cut-off level of the signal Gaussian distribution is small enough, then the differences between the auto-convolutions of limited and not limited signals ought to be negligible in the region $a < r < 2a$, because of the integral character of the convolution operation. If such a limited signal is recorded holographically in nonlinear recording conditions, then in the outer cut-off region during reproduction process there will exist only the noise signals and it will be possible to measure the coordinates of these signals without the background of the desired signal.

In order to estimate the influence of the signal limitation on the measurement accuracy, special filters with the Gaussian power transmittance profile were made and the auto-convolution functions at different cut-off levels were experimentally measured. It was ascertained that if the relative cut-off level does not exceed the value $1/e^2$, then the relative differences between auto-convolutions of limited and not limited signals are within the measurement errors in the region $a < r < 1.5a$.

In the experimental procedure the following conditions were realized:

— the separation conditions assured the separation between the zero-order and first-order diffraction waves up to the waves generated by the 4-th power component of the T_a vs. H polynomial,

— a diffusely scattering glass plate was used as an object,

— the object was illuminated by a spatially filtered TEM_{00} laser mode,

— the diaphragm in the object plane limited the power density distribution at the relative level equal to 0.1,

— the maximal spatial frequencies of the recorded signals were at least 10 times lower than the resolving power of the recording medium.

The assumed exposition parameters were the following:

— the ratio M, defined as a ratio of average power density of the information wave to the power density of the reference wave,

— the average optical density of exposed and developed hologram, defined as

$$D = \lg \frac{T_{e_0}}{T_{e_{av}}}, \tag{45}$$

where T_{e_0} — power transmittance of an unexposed and developed plate,

$T_{e_{av}}$ — average power transmittance of a hologram.

Seven series of holograms vs. exposure time at M values as parameters were done in extremely stable and reproducible conditions. Agfa-Gevaert holographic plates of the type 8E75 were used as a recording medium.

The reproduction scheme was arranged as the reverse configuration in order to obtain a real image of the object at the same angular configuration. The power density distributions in the object plane were analysed by application of a photomultiplier with an aperture limited by a holographic 25 μm pinhole. The results were plotted twice on a $X-Y$ recorder, once at the sensitivity corresponding to the appropriate recording of the general shape of the diagrams, the second time — with sensitivity increased 10 times — in order to get a higher accuracy of the diagram coordinates. One of the records, corresponding to the values $M = 1:3$ and $D = 0.742$, is shown in fig. 7. Because of speckling effects appearing in the records, it was necessary to define averaging lines for proper determining the diagram coordinates.

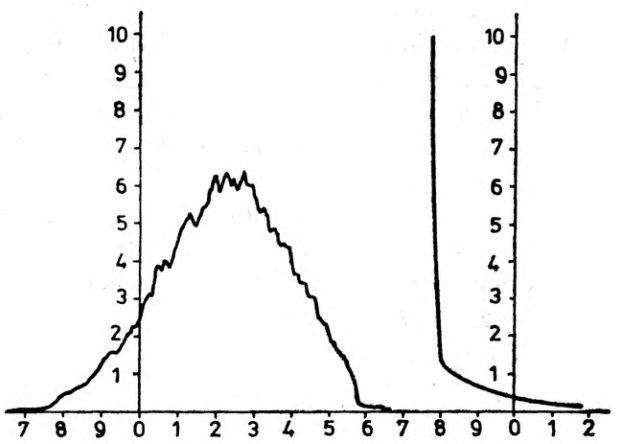

Fig. 7. Power density distribution recorded at $M = 1:3$ and $D = 0.742$

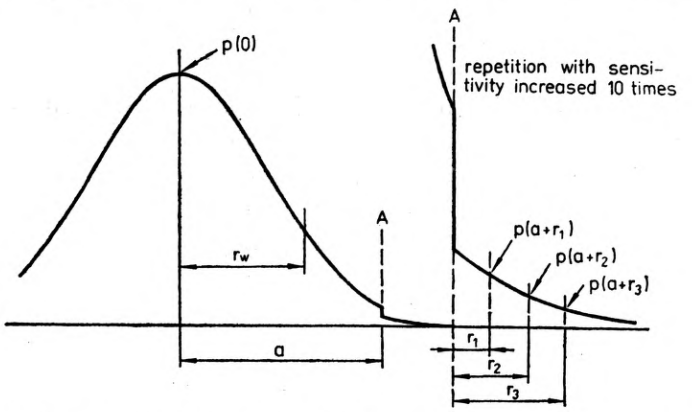

Fig. 8. A scheme of coordinate determination from the experimental records

The figure 8 shows a scheme of coordinate determination from the experimental records. At three values of uniformly spaced radius coordinates, enclosed within the previously mentioned interval $a < a+r_i < 1.5\,a$,

three power densities $p(a+r_i)$ were determined. For every record the pattern of three linear equations

$$p(a+r_i) = p_{N_1}(0)\exp\{-[(a+r_i)/\sqrt{3}r_w]^2\} + p_{N_2}(0)\exp\{-[(a+r_i)/\sqrt{5}r_w]^2\} + p_{N_3}(0)\exp\{-[(a+r_i)/\sqrt{7}r_w]^2\} \tag{46}$$

was solved with respect to $p_{N_i}(0)$ values. In fact, the value $p_{N_3}(0)$ performed a function of a sensor of the shape of T_a vs. H characteristic in the exploited range: when $p_{N_3}(0)$ was within the limits determined by the probable error of coordinate measurements we were assured that the 3-rd power approximation is sufficient. For higher values of $p_{N_3}(0)$ the calculations were not performed.

The value of desired signal $p_S(0)$ was determined as the difference

$$p_S(0) = p(0) - p_{N_1}(0) - p_{N_2}(0). \tag{47}$$

The results calculated for four of the seven different values of the parameter M are shown in fig. 9 vs. the relative average density D of the holograms. The signal and noise values are represented in relative units, the SNR — in decibels.

As a matter of fact, the denominator of the relation (43) ought to include a component, representing the noise developed by a random scattering at the hologram photosensitive layer, in our experiments this noise being not measurable was omitted.

The values D_{opt} and SNR corresponding to the maximal values of $p_{S_{\max}}(0)$ were determined from seven diagrams, like the ones presented in fig. 9. Figure 10 presents the diagrams composed of the above values vs. the ratio M. As can be seen from the diagrams, the maximum maximorum of the hologram diffraction efficiency, with respect to the desired signal only, occurs at

$$M_{\text{opt}} = 0.6, \tag{48}$$

which corresponds to

$$D_{\text{opt opt}} \cong 0.44, \quad \text{or} \quad \frac{T_{e_{\text{opt opt}}}}{T_{e_0}} = 0.36 \tag{49}$$

and

$$\text{SNR}\Big|_{\substack{M_{\text{opt}} \\ D_{\text{opt opt}}}} = 8.5 \text{ dB}. \tag{50}$$

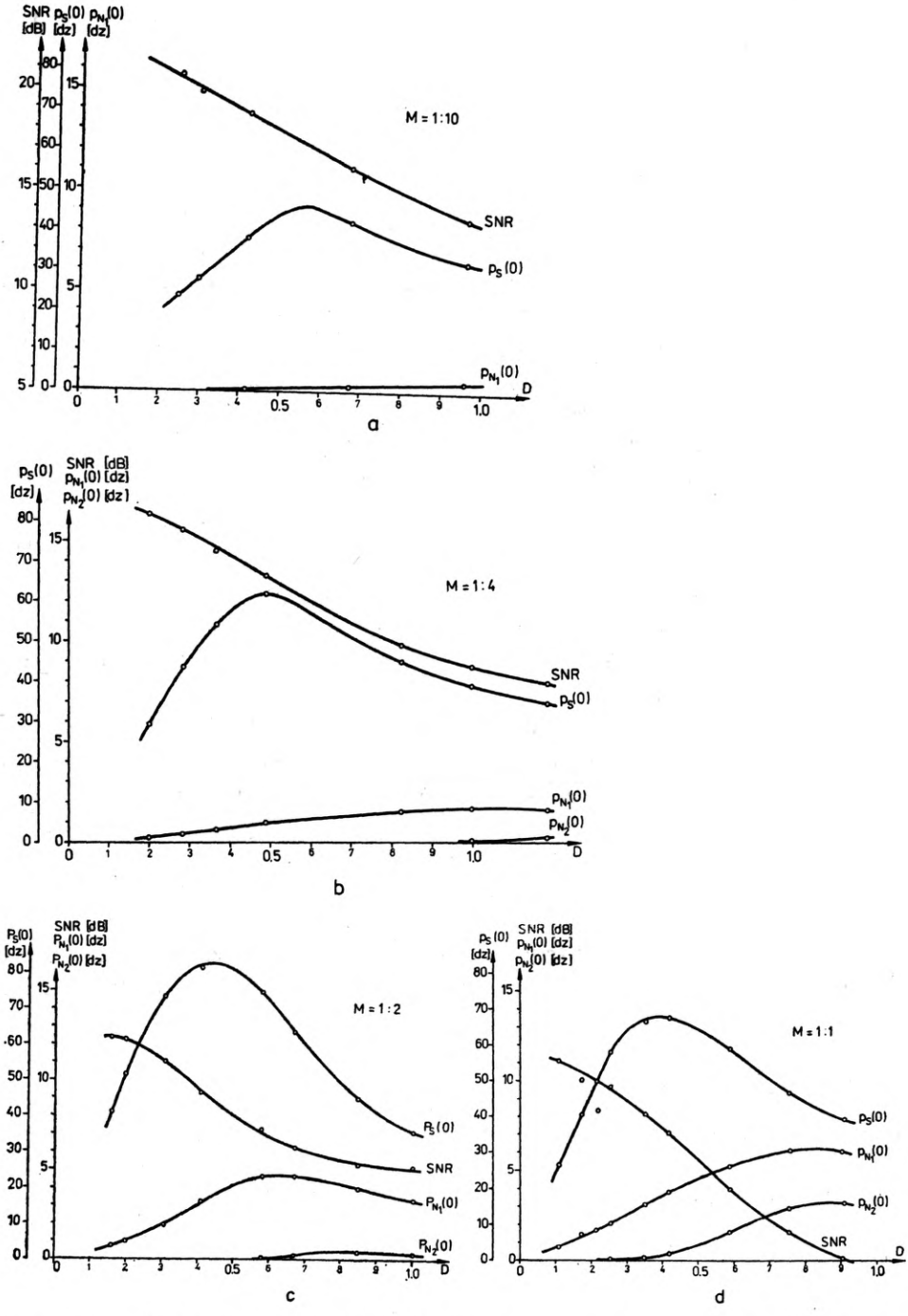

Fig. 9. The calculated results of the desired and noise signals vs. the average hologram density D at the ratios:

a) M=1:10, b) M=1:4, c) M=1:2, d) M=1:1. Here [dz] denotes relative units

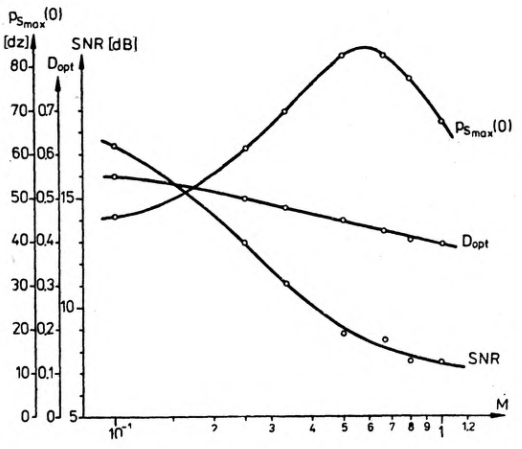

Fig. 10. Composed diagrams of the maximal desired signal $P_{S_{max}}(0)$ and corresponding to it an optimal average hologram density D_{opt} and SNR vs. the ratio M
Here [dz] denotes relative units

5. Conclusions

The experimental results presented in chapter 4 were obtained on the base of a one particular holographic case, so far as the sort of the used photosensitive material, the statistical properties of the recorded waves, and so forth, are concerned. Nevertheless, they contain some attributes, being of a significant importance in all domains of the amplitude holography.

From the diagrams presented in figs. 9 and 10 we can see that

— in every particular case of the amplitude holography there exist optimal values of the ratio M and the average power density D, at which we can reach the maximum of the integral diffraction efficiency,

— within the normally utilized ranges of the M and D values the SNR diminishes monotonically.

The first basic conclusion is that it is disadvantageous to make holograms under conditions: $M > M_{opt}$ and $D > D_{opt\,opt}$, because both the diffraction efficiency and the SNR fall down vs. M and D in these regions. If any doubt exists as to the proper determining of the M or D values it is better to choose rather lower values.

The next problem to be considered is to find a right compromise between the diffraction efficiency and the SNR in the region where M and D are less than their optimal values. Slight lowering of the diffraction efficiency by an appropriate reducing of the M for D values may give the significant gain in the SNR. This fact is of particular importance in the holographic copying processes. In this case the diffraction efficiency of the original hologram has no significance, because the desired value of the M ratio, defining the final diffraction efficiency of the copy, can be determined by the exposure conditions in the copying process. Here rather the

SNR value of the original hologram is of interest, because noises generated by the original hologram are transferred into the copy, reducing the final SNR value of the copy.

References

[1] PAPOULIS A., *System and Transforms with Applications in Optics*, Izd. Mir, Moskva 1971 (in Russian).
[2] KOZMA A., J. Opt. Soc. Am. **56** (1966), 428.

Received March 14, 1980
in revised form May, 2, 1980

Оптические шумы в амплитудной голографии, происходящие от нелинейных свойств регистрирующей среды

Обсуждены вопросы, связанные с возникновением оптических шумов в случаях, в которых голографические сигналы регистрируются в нелинейных амплитудных средах. Доказано, что в голографическом процессе репродукции нелинейная амплитудная голограмма создаёт много нежелаемых сигналов, спектры пространственной частоты которых находятся в области спектра пространственных частот желаемого сигнала. Представлена концепция измерения уровней мощности мешающих сигналов и желаемого сигнала. Описан способ реализации эксперимента, дающего возможность отдельного измерения мощности мешающих сигналов и желаемого сигнала.

Представлены результаты измерений дифракционных коэффициентов полезного действия голограмм и отношения сигнала к шумам в функции параметров экспозиции. Уделено внимание вытекающим из измерений некоторым выводам, представляющим собой общие указания при подборе оптимальных условий экспозиции амплитудных голограмм.